Modelling and Parametric Analysis of the Influence of Vertical Track-defects in Railways

KONSTANTINOS Sp. GIANNAKOS
Civil Engineer, dipl. NTUA, PhD AUTh; Fellow/Life-Member of the Amer. Soc. Civ. Eng. (ASCE)
f. adjunct Professor, University of Thessaly, Civil Engineering Dpt.
Ambassador of WSEAS [= *World Scientific and Engineering Academy and Society*]
108 Neoreion str., Piraeus 18534
GREECE

Abstract: - During the motion of a railway vehicle on a rail, with a rail running table/surface of a random form, the rail running table imposes to the vehicle a forced oscillation. Due to different reasons –manufacturing, corrosion, deterioration etc.- the rail's running surface is not smooth but instead it comprises a lot of defects that give to it a random surface in space. Furthermore, under the primary suspension of the railway vehicle there are the Non-Suspended Masses (N.S.M.) which act without any dumping directly on the track panel. On the contrary the Suspended Masses (S.M.), that are cited above the primary suspension of the vehicle, act through a combination of springs and dashpots on the railway track. A part of the track mass is also added to the Non-Suspended Masses, which participates in their motion. The longitudinal vertical defects of the Track, which play a key role, on the dynamic component of the acting loads on the railway track-panel, and, consequently, -due to the principle action=reaction- on the dynamic component of the action/reaction of the railway track on the railway vehicle, are modelled and analyzed parametrically using the second order differential equation of motion. The parametric investigation is performed for the cases of defects of short and long wavelength.

Key-Words: - railway track; dynamic stiffness; actions; reactions; loads; deflection; subsidence; eigenperiod; forcing period.

Received: June 14, 2025. Revised: September 27, 2025. Accepted: October 25, 2025. Published: January 26, 2026.

1 The System 'Vehicle-Track' in Railways

The railway track is usually modeled as a continuous beam on elastic support. Train circulation is a random dynamic phenomenon and, depending on the different frequencies of the loads it imposes, there is a corresponding response of the track superstructure. At the instant, when an axle passes from the location of a sleeper, a random dynamic load is applied on the sleeper. The theoretical approach for the estimation of the dynamic loading of a sleeper requires the analysis of the total load acting on the sleeper to individual component loads-actions, which, in general, can be divided into:

(a) the static component of the load, and the relevant reaction/action per support point of the rail (sleeper) and

(b) the dynamic component of the load, and the relevant reaction/action per support point of the rail (sleeper).

The static component of the load on a sleeper, in the classical sense, refers to the load undertaken by the sleeper when a vehicle axle at standstill is situated

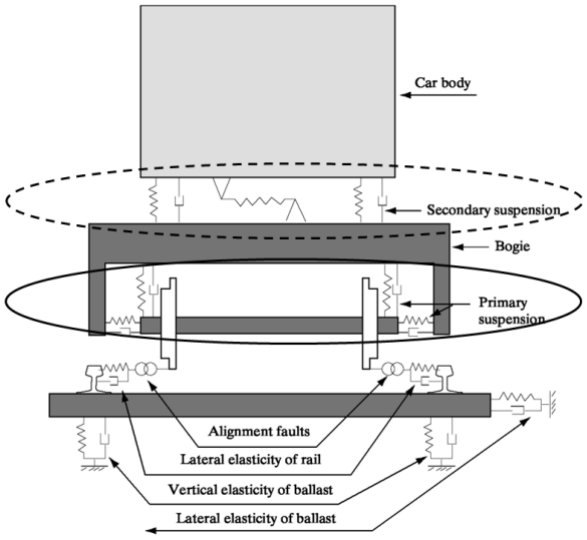

Figure 1a. "Railway Vehicle - Railway Track", in a cross-section with the parts of the vehicle, the track and the approach/simulation of the defects and the elasticity of the Track-Vehicle system.

static load is further analyzed into individual component loads: the static reaction/action on a sleeper due to wheel load and the semi-static Reacti-

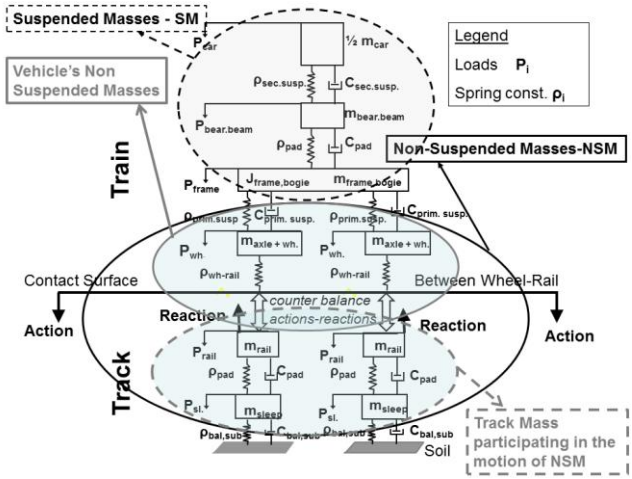

Figure 1b. The "Railway Vehicle-Railway Track" system, simulated as an Ensemble of Springs and Dashpots.

Figure 2. (Upper illustration) MLW 500-series diesel locomotive of the Greek railways, with three-axle bogies; the three-axle bogie is marked with the black ellipse. In Greece, $Q_{max.}$ 22,5 t/axle and NSM_{max} 5,08 t/axle. (Lower illustration) A three-axle bogie in detail: in the white ellipse the primary suspension and in the black ellipse the secondary suspension are depicted.

on/Action due to cant deficiency ([1], [29]). The dynamic component of the load of the track depends on the mechanical properties (stiffness, damping) of the system "vehicle-track" (Fig. 1), and on the excitation caused by the vehicle's motion on the track.

The response of the Track to the aforementioned excitation results in increase of the static component of the load on the superstructure. The dynamic component of the load is primarily caused by the motion of the vehicle's Non-Suspended (Unsprung) Masses, which are excited by track geometry defects -esecially the vertical ones-, and, to a smaller degree, by the effect of the Suspended (sprung) Masses.

In order to formulate the theoretical equations (of motion) for the calculation of the dynamic component of the load, the statistical probability of occurrence/exceedance of the calculated load -in real conditions- should be considered, so that the corresponding equations would refer to the standard deviation (variance) of the load ([1]]; [2]).

The track defects are classified as (a) short wave-lenth defects and (b) long wavelength defects (see [3]). *The real defects are consecutive, not isolated, and random*. In the present paper the dynamic component of the acting load, for the short and long wave-length defects, is investigated through the second order differential equation of motion of the Non-Suspended Masses of the Vehicle and specifically the transient response of the reaction-action on each support point (sleeper) of the rail.

2 The Motion of a Railway Vehicle on a Railway Track

The railway vehicles consist of (a) the car-body, (b_1) the *primary suspension* between the bogie-frame and the axle(s), (b_2) *the secondary suspension* between the bogie-frame and the car-body and (c) the axles with the wheels (Fig. 2). In general, the mass of the (c) case is situated under the primary suspension of the vehicle and is the Non-Suspended Mass of the vehicle. The heaviest vehicles are the locomotives, which are "motive units" and have electric motors whose a portion of its mass is suspended by the frame of the bogie and another portion of its mass is based on the axles directly. In Fig. 2-upper a locomotive with three-axle bogie is depicted, while the three axle bogie with the springs of the primary and secondary suspensions is depicted in Fig. 2-lower.

There are electric motors suspended totally from the frame of the bogie but -in the case of diesel-locomotives- they are suspended partly on the frame of the bogie at their one end and partly based on the axle at their other end. In the second case the electric motor is semi-suspended (Fig. 3) and a part of it is considered also as Non-Suspended Mass, as it will be clarified below.

If we try to approach mathematically the motion of a vehicle on a railway track, we will end up with the model shown in Fig. 1b, where both the vehicle and the railway track are composed of an ensemble of masses, springs and dashpots.

As we can observe, the car-body is based on the secondary suspension that includes two sets of

"springs-dashpots", seated on the frame of the bogie (Fig. 1-left and Fig. 3-right). The loads are transferred to the truss and the side frames of the bogie-frame. Underneath the bogie there is the primary suspension, through which the bogie is seated onto the carrying axles and the wheels. Below the contact surface, between the wheel and the rail, the railway track also consists of a combination of masses-springs-dampers that simulates the rail, the sleepers, the elastic pad, the rail fastenings, the ballast and the ground.

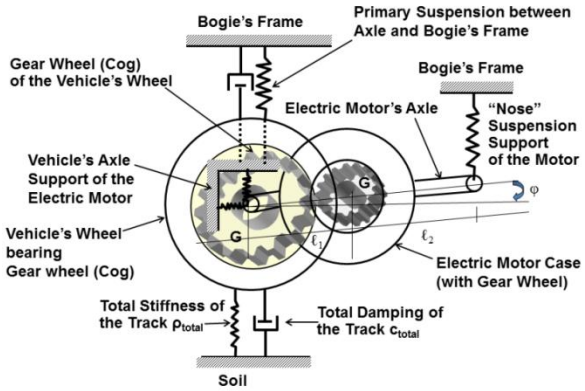

Figure 3. Schematic depiction of an Electric Motor "semi-suspended" from the bogie's frame at one end ("Nose" suspension) and supported on the vehicle's axle at the other end.

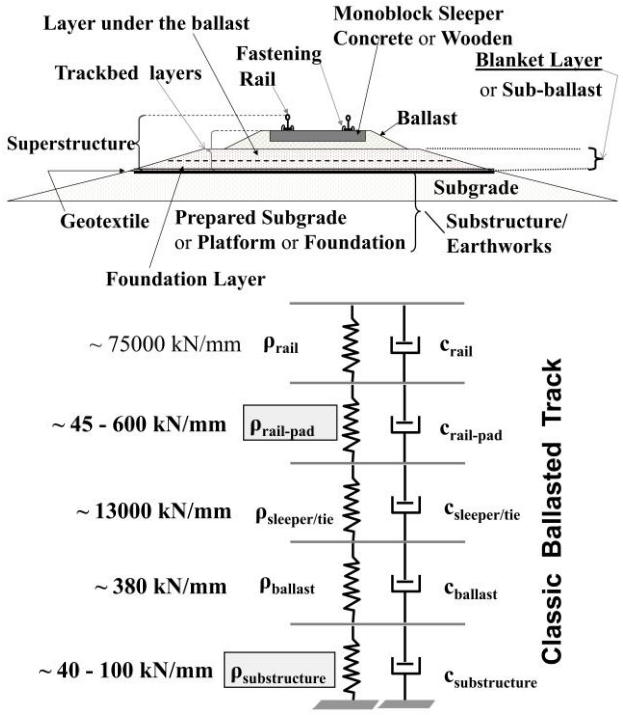

Figure 4. (Upper illustration) Cross-section of Ballasted Track as a multi-layered structure.; (Lower illustration) Characteristic Values of Static Stiffness Coefficients of each layer.

The masses of the railway vehicle located under the primary suspension (axles, wheels and a percentage of the electric motor weight in the case of locomotives) are the Non-Suspended Masses (N.S.M.) of the Vehicle, that act directly on the railway track without any damping at all. Furthermore, a section of the track mass (m_{TRACK}) also participates in the motion of the vehicle's Non-Suspended Masses, which also highly aggravates the stressing on the railway track (and on the vehicle too) ([1]; [2]].

The defects of the rail running table, a wave in space of random nature, impose a forced oscillation on the Non-Suspended Masses of the vehicle; their form constitutes a forcing excitation. From the form of the rail running table the forcing period or frequency can be calculated.

The remaining vehicle masses are called Suspended Masses (S.M.) or Sprung Masses: the car-body, the secondary suspension, the frame of the bogie, a part of the electric motor's weight and the primary suspension.

3 Modelling the Railway Track to formulate the 2nd Order Differential Equation of Motion

The theoretical analysis of a railway track is based mainly in Winkler's theory ([4]), which models it as an infinite beam on elastic foundation. In European literature it is also referred to as Zimmermann's theory ([5]). The elastic foundation of the railway track can be simulated by a large number of closely spaced translational springs and the following equation is valid ([3]; [6]):

$$EJ\frac{\partial^4 y}{\partial x^4}+\rho_1\cdot\frac{\partial^2 y}{\partial x^2}+k_1\cdot z=0 \qquad (3.1)$$

in the absence of external force, or:

$$EJ\frac{\partial^4 y}{\partial x^4}+\rho_1\cdot\frac{\partial^2 y}{\partial x^2}+k_1\cdot y=-Q\cdot\delta(x) \qquad (3.2)$$

with the presence of external force.

In these equations y is the deflection of the beam, ρ_1 is the mass of the track participating in the motion, k_1 the viscous damping of the track, J is the moment of inertia of the rail, E is the modulus of elasticity of the rail, Q the force/load from the wheel (when the force is present) and δ(x) the deflection of the rail at the contact point between wheel and rail.

The solution of equations (3.1) and (3.2) becomes challenging if we want to take into account all the parameters according to professor J. Alias ([7]). However, if we make some simplifying hypotheses,

we will be able to approximate the influence of certain parameters, provided that we will verify the theoretical results with experimental measurements. Apparently having in mind the tests on Track under operation/circulation, performed by the European Railways and the International Union of Railways (U.I.C. or UIC in French), professor J. Eisenmann states already since 1988 that, the -based on Zimmermann's theory- methods *give results corresponddent at the average of the measured on track values, for track's loading and stressing, as well as track's deflection* ([8]). Consequently, the level of the maximum values is dependent on the possibility of occurrence -mainly- of the dynamic component of the acting load.

The most widely used theory (referred to as the Zimmermann theory) based on Winkler analysis examines the track as a beam on elastic support.

$$\frac{d^4y}{dx^4} = -\frac{1}{E\cdot J}\cdot\frac{d^2M}{dx^2} \tag{3.3}$$

where y is the deflection of the rail, M is the bending moment, J is the moment of inertia of the rail, and E is the modulus of elasticity of the rail. From the formula above it is derived that the reaction of a sleeper R_{static} (that is of each support point of the track) acting on the railway vehicle is:

$$R_{stat} = \frac{Q_{wheel}}{2\sqrt{2}}\cdot\sqrt[4]{\frac{\ell^3\cdot\rho_{total}}{E\cdot J}} \Rightarrow \frac{R_{stat}}{Q_{wheel}} = \bar{A} = \bar{A}_{stat} = \frac{1}{2\sqrt{2}}\cdot\sqrt[4]{\frac{\ell^3\cdot\rho_{total}}{E\cdot J}} \tag{3.4a}$$

where Q_{wheel} the static wheel load, ℓ the distance among the sleepers, E and J the modulus of elasticity and the moment of inertia of the rail, R_{stat} the static reaction/action on the sleeper, and ρ reaction coefficient of the sleeper which is defined as: ρ=R/y, and is a quasi-coefficient of the track elasticity (stiffness) or a spring constant of the track. The track consists of a sequence of materials (substructure, ballast, sleeper, elastic pad/ fastening, rail), that are characterized by their individual coefficients of elasticity (static stiffness coefficients) ρ_i [see Fig.4-Lower].

Hence, for the track:

$$\rho_i = \frac{R}{y_i} \Rightarrow y_i = \frac{R}{\rho_i} \Rightarrow y_{total} = \sum_{i=1}^{\nu} y_i \Rightarrow y_{total} = \sum_{i=1}^{\nu}\frac{R}{\rho_i} \Rightarrow$$
$$y_{total} = R\cdot\sum_{i=1}^{\nu}\frac{1}{\rho_i} \Rightarrow \frac{1}{\rho_{total}} = \sum_{i=1}^{\nu}\frac{1}{\rho_i} \Rightarrow \tag{3.4b}$$
$$\frac{1}{\rho_{total}} = \sum_{i=1}^{\nu}\frac{1}{\rho_i} = \frac{1}{\rho_{rail}} + \frac{1}{\rho_{pad}} + \frac{1}{\rho_{sleeper}} + \frac{1}{\rho_{ballast}} + \frac{1}{\rho_{subgrade}}$$

where ν is the number of various layers of materials that exist: rail, elastic pad, sleeper, ballast, subgrade. The semi-static Action is produced by the centrifugal acceleration exerted on the wheels of a vehicle that is running in a curve with cant deficiency, given by [see [29]]:

$$Q_\alpha = \frac{2\cdot\alpha\cdot h_{CG}}{e^2}\cdot Q_{wheel} \tag{3.4c}$$

where α is the cant deficiency, h_{CG} the height of the center of gravity of the vehicle from the rail and e the gauge.

The total Static+Semi-Static Reaction/Action ($R_{stat\text{-}total}$) on each support point of the rail is given by Eqn. (3.4a) where:

$Q_{wheel} = Q_{static} + Q_a$

$$\frac{R_{stat}}{Q_{wheel}+Q_\alpha} = \bar{A} = \bar{A}_{stat} = \frac{1}{2\sqrt{2}}\cdot\sqrt[4]{\frac{\ell^3\cdot\rho}{E\cdot J}} \Rightarrow$$
$$R_{stat} = \left(Q_{wheel}+Q_\alpha\right)\cdot\frac{1}{2\sqrt{2}}\cdot\sqrt[4]{\frac{\ell^3\cdot\rho}{E\cdot J}} = \left(Q_{wheel}+Q_\alpha\right)\cdot\bar{A}_{stat} \tag{3.4d}$$

If the acting load is determined, then the Action-Reaction on each support point (sleeper) of the rail will be determined too. The system “railway vehicle-railway track” operates based on the classical principles of physics: equivalence of Action-Reaction between the vehicle and the track. It is a dynamic stressing of random, vertical form.

The loading of the railway track from a moving vehicle consists of:

(a) the static component of the load (static load of the vehicle’s axle), as given by the rolling stock’s producer.

(b) the semi-static component of the load (due to cant or superelevation deficiency at curves, which results in non-compensated lateral acceleration).

(c) the component of the load from the Non-Suspended Masses of the vehicle (the masses that are not damped by any suspension, because they are under the primary suspension of the vehicle), which is a dynamic load by its nature and

(d) the component of the load from the Suspended Masses of the vehicle, that is a damped force component of the total action on the railway track and it is also a dynamic load.

On each support point of the rail (sleeper) a reaction/action is applied due to the distribution of the acting load to the adjacent sleepers (support points of the rail) because of the total elasticity/total static stiffness coefficient of the track. For the static and the semi-static components of the load these reactions/actions are given from the Eqns (3.4a) and (3.4d), as derived from the solution of the differential equation of motion. But for the dynamic component of the load a modelling of the motion of the Non-Suspended Masses should be performed.

Finally, the differential equation is transformed to the following equation connecting the deflection of

the continuous beam and the bending moment ([3]; [6]) as given by Eqn. (3.3).

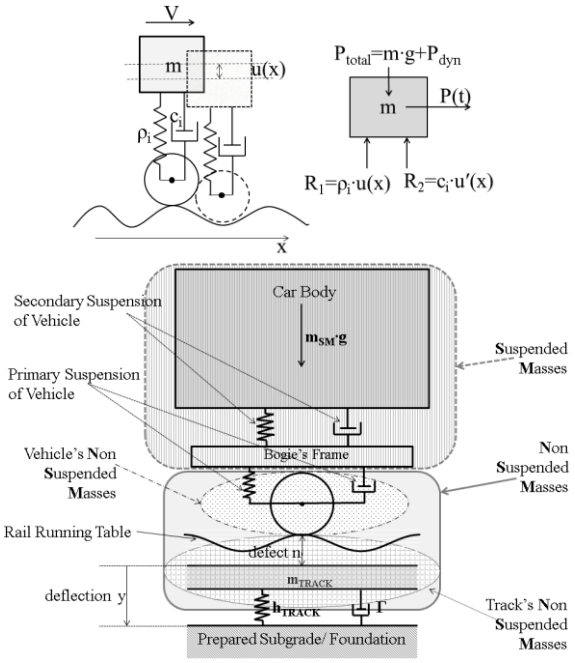

Figure 5. Schematic mapping of a vehicle/car on a Raiway Track: (Upper) elementary graph; (lower) m_{NSM} the Non-Suspended Masses (under the primary suspension) of the vehicle (the not depicted secondary suspension is between the bogie-frame and the car-body); m_{TRACK} the mass of the track that participates in the motion of the Non-Suspended Masses (m_{NSM}); m_{SM} the Suspended Masses of the vehicle/car-body (above the primary suspension); Γ damping constant of the track; h_{TRACK} the total dynamic stiffness coefficient of the track; n the fault ordinate of the rail running table, and y the deflection of the track. The dynamic component is owed to the NSM and the SM; [cf. [12]]. [SOURCE [28]]

4 Modelling the Motion of the Non-Suspended Masses on a Railway Track to formulate the 2nd Order Differential Equation of Motion

The Suspended (sprung) Masses of the vehicle – masses situated above the primary suspension– create forces with very small influence on the wheel's trajectory and on the system's excitation. This enables the simulation of the track as an elastic media with damping, as shown in Fig. 5 (see relevantly [3]; [10]), and also the modelling of the motion of the Non-Suspended Masses of a railway vehicle on it. Forced oscillation is caused by the irregularities of the rail running table (like an input random signal) - which are represented by n-, in a gravitational field with acceleration g, whilst the total deflection of the rail's running table, due to the wheel's passage, is y. As already described, there are two suspensions on the vehicle for passenger comfort purposes: primary and secondary suspension. Moreover, a section of the mass of the railway track participates in the motion of the Non-Suspended (Unsprung) Masses of the vehicle. These Masses are situated under the primary suspension of the vehicle.

If the random excitation (track irregularities) is given, it is difficult to derive the response, unless the system is linear and invariable. In this case the input signal can be defined by its spectral density and from this we can calculate the spectral density of the response. The theoretical results confirm and explain the experimental verifications performed in the former British railway network ([11]; relevant results in [7], p.39, 71 and also in [3]; [6]).

The equation for the interaction between the vehicle's axle and the track-panel becomes ([3]; [6]; [12]):

$$\left(m_{NSM}+m_{TRACK}\right)\cdot\frac{d^2y}{dt^2}+\Gamma\cdot\frac{dy}{dt}+h_{TRACK}\cdot y=$$

$$=-m_{NSM}\cdot\frac{d^2n}{dt^2}+\left(m_{NSM}+m_{SM}\right)\cdot g \qquad (4.1a)$$

where: m_{NSM} the Non-Suspended (Unsprung) Masses of the vehicle, m_{TRACK} the mass of the track that participates in the motion, m_{SM} the Suspended (Sprung) Masses of the vehicle that are cited above the primary suspension of the vehicle, Γ damping constant of the track (for its calculation see [13]; [14]), h_{TRACK}=ρdynamic the total dynamic stiffness coefficient of the track, n the fault ordinate of the rail running table and y the total deflection of the track, and:

$$h_{TRACK}=\rho_{total-dynamic}=2\sqrt{2}\cdot\sqrt[4]{E\cdot J\cdot\frac{\rho_{total-static}}{\ell}} \qquad (4.1b)$$

The phenomena of the wheel-rail contact and of the wheel hunting, particularly the equivalent conicity of the wheel and the forces of pseudo-glide, are non-linear. In any case the use of the linear system's approach is valid for speeds lower than the Vcritical≈500 km/h. The integration for the non-linear model (wheel-rail contact, wheel-hunting and pseudoglide forces) is performed through the Runge Kutta method ([7], p.94-95, 80; [15], p.98; [16], p.171, 351). Consequently, for all operational speeds in High-Speed Railway Lines up to now the linear model, which we use, is quite reliable.

The defects of the rail running table are categorized in short wavelength defects and long wavelength defects. The analysis and investigation of the Eqn (4.1a), for consecutive short wavelength

defects (e.g. the rail surfaces corrugation, of wavelength of some centimeters), was presented in [3]. The long wavelength defects are difficult to be measured, since sometimes, their wavelength overpass the measurements' base, which is determined by the distance between the measuring vehicle's axles. In this article the long wavelength defects are modelled, analyzed and investigated.

The dynamic component of the acting load consists of the action due to the Sprung or Suspended Masses (SM) and the action due to the Unsprung or Non-Suspended Masses (NSM) of the vehicle. To the latter a section of the track mass is added, that participates in its motion ([13]; [14]). The Suspended (Sprung) Masses of the vehicle –masses situated above the primary suspension (Fig. 1)– apply forces with very small influence on the trajectory of the wheel and on the excitation of the system. This enables the simulation of the track as an elastic media with damping which takes into account the rolling wheel on the rail running table ([3]; [17]; [18]). Forced oscillation is caused by the irregularities of the rail running table (simulated by an input random signal) –which are represented by n–, in a gravitational field with acceleration g. There are two suspensions on the vehicle for passenger comfort purposes: primary and secondary suspension. Moreover, a section of the mass of the railway track participates in the motion of the Non-Suspended (Unsprung) Masses of the vehicle. These Masses are situated under the primary suspension of the vehicle.

We approach the matter considering that the rail running table contains a longitudinal fault/ defect of the rail surface. In the above equation, the oscillation of the axle is damped after its passage over the defect. Viscous damping, due to the ballast, enters the above equation under the condition that it is proportional to the variation of the deflection dy/dt. To simplify the investigation, if the track mass (for its calculation see ([13]; [14]) is ignored -in relation to the much larger Vehicle's Non-Suspended Mass- and bearing in mind that y+n is the total subsidence of the wheel during its motion (since the y and n are added algebraically), we can approach the problem of the random excitation, based on a cosine defect (V< Vcritical=500 km/h):

$$\eta = a \cdot \cos \omega t = a \cdot \cos\left(2\pi \cdot \frac{V \cdot t}{\lambda} \right) \qquad (4.2)$$

The second order differential equation of motion is:

$$m_{NSM} \frac{d^2 z}{dt^2} + \Gamma \cdot \frac{dz}{dt} + h_{TRACK} \cdot z = -m_{NSM} \cdot a \cdot \omega^2 \cdot \cos(\omega t) \qquad (4.3)$$

The complete solution of which using polar coordinates is ([6], p.199 and ch.3):

$$z = \underbrace{A \cdot e^{-\zeta \omega_n t} \cdot \sin\left(\omega_n t \sqrt{1-\zeta^2} - \varphi \right)}_{transient-part} + \underbrace{a \cdot B \cdot \cos(\omega t - \varphi)}_{steady-state-part} \qquad (4.4)$$

where, the first term is the *transient part* and the second part is the *steady state part*.

5 Mathematical Analysis of the System 'Vehicle-Track', beginning from an Isolated Defect of the Railway Track

The modelling -described above- gives equations to calculate the actions on track depending on the parametrical analysis of the conditions on the railway track. In order to approach the long wavelength defects, we begin by trying to relate the depth (sagittal) of an isolated defect to the dynamic component of the load. We neglect the steady state part of Eqn (4.4):

$$a \cdot B \cdot \cos(\omega t - \varphi) \qquad (5.1)$$

We focus herein on the transient part of the load, that is the term:

$$A \cdot e^{-\zeta \omega_n t} \cdot \sin\left(\omega_n t \sqrt{1-\zeta^2} - \varphi \right) \qquad (5.2)$$

We investigate this term for ζ=0. The theoretical analysis for the additional -to the static and semi-static component- dynamic component of the load due to the Non-Suspended Masses and the Suspended Masses of the vehicle, leads to the examination of the influence of the Non-Suspended Masses only, since the frequency of oscillation of the Suspended Masses is much smaller than the frequency of the Non-Suspended Masses. If m_{NSM} represents the Non-Suspended Mass, m_{SM} the Suspended Mass and m_{TRACK} the Track Mass participating in the motion of the Non-Suspended Masses of the vehicle, the differential equation is (with no damping ζ=0):

$$m_{NSM} \cdot \frac{d^2 z}{dt^2} + h_{TRACK} \cdot z = m_{NSM} \cdot g \Rightarrow$$

$$\left(m_{NSM} + m_{TRACK} \right) \cdot \frac{d^2 z}{dt^2} + h_{TRACK} \cdot z = m_{NSM} \cdot g \qquad (5.3)$$

where: g the acceleration of gravity and h_{TRACK}, the total dynamic stiffness coefficient of track, given by Eqn. (4.1b).

where the track mass m_{TRACK} that participates in the motion of the Non-Suspended (Unsprung) Masses of the Vehicles, ρ_{total} the total static stiffness coefficient of the track, ℓ the distance among the sleepers, E, J the modulus of elasticity and the moment of inertia of the rail, m_0 the unitary mass of track (per unit of length of the track).

For a comparison of the theoretical track mass to measurement results refer to [13]; [14]. The particular solution of the differential Eqn (5.3) corresponds to the static action of the weight of the wheel:

$$z = \frac{m_{TRACK} \cdot g}{h_{TRACK}} \qquad (5.3a)$$

We assume that the rolling wheel runs over an isolated sinusoidal defect of length λ of the form:

$$n = \frac{a}{2} \cdot \left(1 - \cos\frac{2\pi x}{\lambda}\right) = \frac{a}{2} \cdot \left(1 - \cos\frac{2\pi V t}{\lambda}\right)$$

where n is the ordinate of the defect. Consequently, the ordinate of the center of inertia of the wheel is $n+z$. Defining τ_1 as the time needed for the wheel to pass over the defect at a speed V:

$$\tau_1 = \frac{\lambda}{V} \quad \text{, then:}$$

$$m_{NSM} \cdot \frac{d^2}{dt^2}(z+n) + m_{TRACK} \cdot \frac{d^2 z}{dt^2} + h_{TRACK} \cdot z = 0 \Rightarrow$$

$$\Rightarrow (m_{NSM} + m_{TRACK}) \cdot \frac{d^2 z}{dt^2} + h_{TRACK} \cdot z = -m_{NSM} \cdot \frac{d^2 n}{dt^2} =$$

$$= -m_{NSM} \cdot \frac{2a\pi^2}{\tau_1^2} \cdot \cos\frac{2\pi t}{\tau_1}$$

Since:

$$\frac{dn}{dt} = \frac{a}{2} \cdot \frac{2\pi V}{\lambda} \cdot \sin\frac{2\pi V t}{\lambda} = \frac{a}{2} \cdot \frac{2\pi\lambda}{\lambda \cdot \tau_1} \cdot \sin\frac{2\pi V t}{\lambda} \Rightarrow$$

$$\frac{dn}{dt} = \frac{a}{2} \cdot \frac{2\pi}{\tau_1} \cdot \sin\frac{2\pi V t}{\lambda} \Rightarrow$$

$$\frac{d^2 n}{dt^2} = -\frac{a}{2} \cdot \left(\frac{2\pi}{\tau_1}\right)^2 \cdot \cos\frac{2\pi V t}{\lambda} = -\frac{a}{2} \cdot \left(\frac{2\pi}{\tau_1}\right)^2 \cdot \cos\frac{2\pi\lambda t}{\lambda \cdot \tau_1} \Rightarrow$$

$$\frac{d^2 n}{dt^2} = -\frac{2a\pi^2}{\tau_1^2} \cdot \cos\frac{2\pi t}{\tau_1}$$

Where: $x = V \cdot t, \quad \omega_1 = 2 \cdot \frac{\pi \cdot V}{\ell} = \frac{2\pi}{T}, \quad \omega_n^2 = \frac{h_{TRACK}}{m_{NSM}}$

and ω_1 the cyclic frequency of the external force and ω_n the natural frequency.

The additional dynamic component of the load due to the motion of the wheel is:

$$-m_{NSM} \cdot (z'' + n'') = h_{TRACK} \cdot z + m_{TRACK} \cdot z'' \qquad (5.4)$$

To solve Eqn (5.3) we divide by (m_{NSM}+m_{TRACK}):

$$\frac{d^2 z}{dt^2} + \frac{h_{TRACK}}{(m_{NSM} + m_{TRACK})} \cdot z = -\frac{m_{NSM}}{(m_{NSM} + m_{TRACK})} \cdot \frac{2a\pi^2}{\tau_1^2} \cdot \cos\frac{2\pi t}{\tau_1}$$

(5.5a)

The differential equation of motion, for an undamped forced harmonic motion is ([19]; [20]):

$$m \cdot \ddot{z} + kz = p_0 \cos(\omega_1 t) \Rightarrow$$

$$\ddot{z} + \frac{k}{m} z = \frac{p_0}{m} \cos(\omega_1 t) = \omega_n^2 \cdot \frac{p_0}{k} \cos(\omega_1 t) \qquad \textbf{(5.5b)}$$

where: $\omega_n^2 = \frac{k}{m} \Rightarrow m = \frac{k}{\omega_n^2}$

Eqn (5.5a) is quite the same as Eqn (5.5b), *since k is the spring constant and m the mass*.

The complete solution is (*see Annex 1*):

$$z(t) = \frac{p_0}{k} \cdot \frac{1}{1 - \left(\frac{\omega_1}{\omega_n}\right)^2} \cdot \left[\underbrace{\cos(\omega_1 t)}_{steady-state} - \underbrace{\cos(\omega_n t)}_{transient-part}\right] \qquad (5.6)$$

where: k=h_{TRACK}, m=m_{NSM}+m_{TRACK} and:

$$\omega_n^2 = \frac{h_{TRACK}}{m_{NSM} + m_{TRACK}}, \quad p_0 = -\frac{2 \cdot \alpha \cdot \pi^2 \cdot m_{NSM}}{\tau_1^2}$$

The general solution of Eqn (15) is:

$$z(t) = -\underbrace{\frac{2 \cdot \alpha \cdot \pi^2 \cdot m_{NSM}}{\tau_1^2}}_{p_0} \cdot \frac{1}{h_{TRACK}} \cdot \frac{1}{1 - \left(\frac{\omega_1}{\omega_n}\right)^2} \cdot \left[\underbrace{\cos(\omega_1 t)}_{steady-state} - \underbrace{\cos(\omega_n t)}_{transient-part}\right] =$$

$$= \frac{\alpha}{2} \cdot \frac{m_{NSM}}{(m_{NSM} + m_{TRACK})} \cdot \frac{1}{1 - \left(\frac{\omega_n}{\omega_1}\right)^2} \cdot \left[\underbrace{\cos(\omega_1 t)}_{steady-state} - \underbrace{\cos(\omega_n t)}_{transient-part}\right]$$

and:

$$z(t) = -\frac{1}{2} \cdot \frac{4 \cdot \pi^2}{\underbrace{\tau_1^2}_{\omega_1^2}} \cdot \frac{\alpha \cdot m_{NSM}}{\underbrace{\omega_n^2 \cdot (m_{NSM} + m_{TRACK})}_{h_{TRACK}}} \cdot \frac{1}{1 - \left(\frac{\omega_1}{\omega_n}\right)^2} \cdot \left[\underbrace{\cos(\omega_1 t)}_{steady-state} - \underbrace{\cos(\omega_n t)}_{transient-part}\right] =$$

$$= \frac{\alpha}{2} \cdot \frac{m_{NSM}}{(m_{NSM} + m_{TRACK})} \cdot \frac{1}{1 - \left(\frac{\omega_n}{\omega_1}\right)^2} \cdot \left[\underbrace{\cos(\omega_1 t)}_{steady-state} - \underbrace{\cos(\omega_n t)}_{transient-part}\right] \qquad (5.7)$$

where, $T_n = 2\pi/\omega_n$ the period of the free oscillation of the wheel circulating on the rail and $T_1 = 2\pi/\omega_1$ the necessary time for the wheel to run over a defect of wavelength λ: $T_1 = \lambda/V$. Consequently, $T_n/T_1 = \omega_1/\omega_n$.

From Eqn (5.7):

$$\frac{(m_{NSM} + m_{TRACK})}{m_{NSM}} \cdot z(t) = \alpha \cdot \frac{1}{2} \cdot \frac{1}{1 - \left(\frac{\omega_n}{\omega_1}\right)^2} \cdot \left[\underbrace{\cos(\omega_1 t)}_{steady-state} - \underbrace{\cos(\omega_n t)}_{transient-part}\right]$$

(5.8)

We can investigate Eqn (5.8) after a parametric analysis by variating parameters: for given values of $T_n/T_1 = \omega_1/\omega_n$ and for given value of V (for example equal to 1) the time period T_1 is proportional to μ=0.1, 0.2, … 1.0 of defect λ (where λ is the defect's wavelength). Equation (5.8) is transformed:

$$\left[\frac{(m_{NSM} + m_{TRACK})}{m_{NSM}} \cdot z(t) \cdot \frac{1}{\alpha}\right] = \frac{1}{2} \cdot \frac{1}{1 - (n)^2} \cdot \left[\underbrace{\cos(\omega_1 t)}_{steady-state} - \underbrace{\cos(n \cdot \omega_1 t)}_{transient-part}\right] =$$

$$= \frac{1}{2} \cdot \frac{1}{1 - (n)^2} \cdot \left[\underbrace{\cos(2\pi \cdot \mu)}_{steady-state} - \underbrace{\cos(n \cdot 2\pi \cdot \mu)}_{transient-part}\right] \qquad (5.9)$$

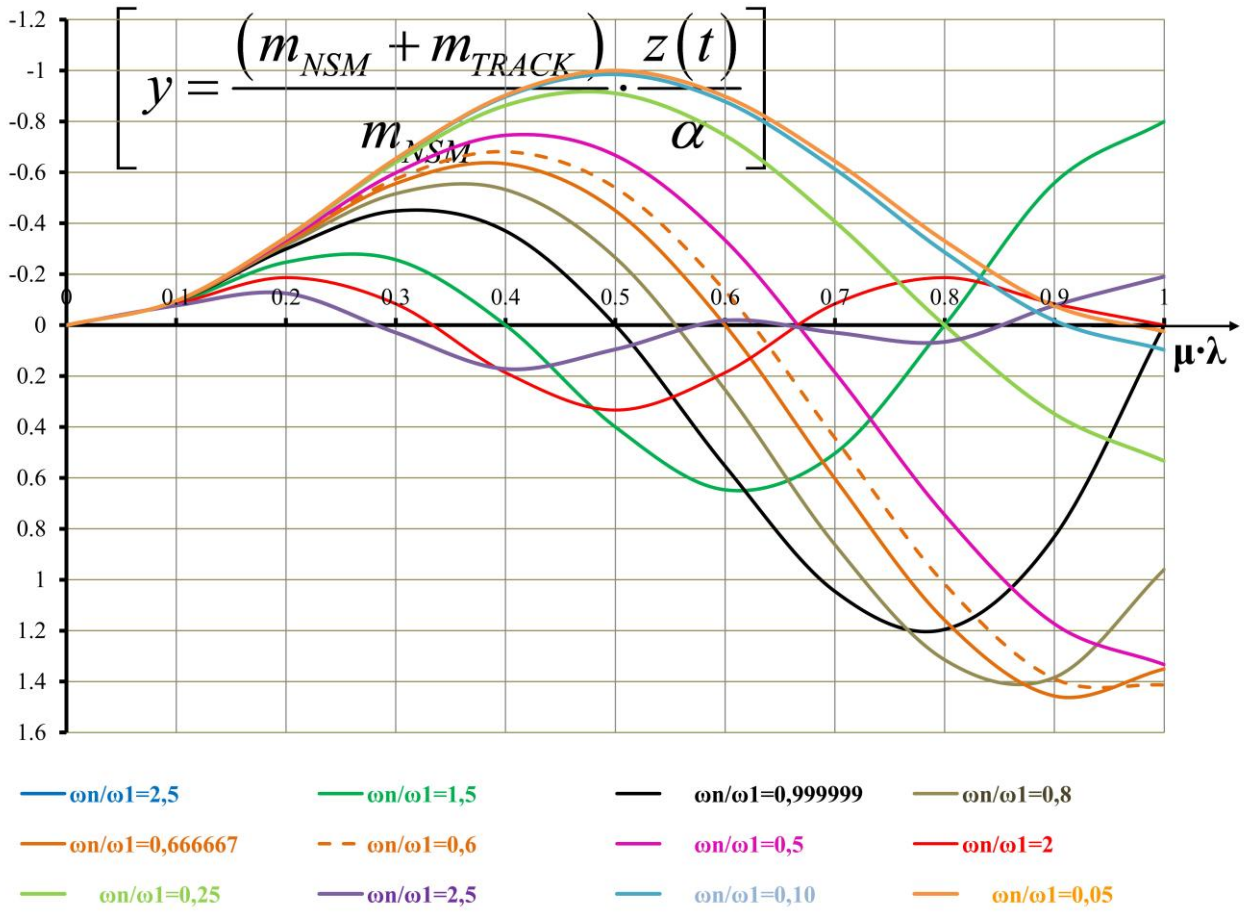

Figure 6. Depicting Eqn (5.9) on a graph (in a scale). For the deflection [z] (Eqn 5.3a) due to a defect of short or long wavelength: on the Horizontal Axis the percentage of the wavelength λ of the defect is depicted. On the Vertical Axis the first term [y=kz] of Eqn (5.9), inside the brackets, is depicted [see §6].

where $n=\omega_n/\omega_1$, $\omega_1=\lambda/V$ and we examine values of $\mu\cdot\lambda=0,\ 0.1\lambda,\ 0.2\lambda,\ldots,\ 0.8\lambda,\ 0.9\lambda,\ \lambda$, for discrete values of $n=\omega_n/\omega_1$ ($=T_1/T_n$) and μ a percentage of the wavelength λ. In Fig. 6 the equation (5.9) is depicted.

In real Railway-Tracks the recordings of defects are distorted by the measurements of the Track Recording Cars and their correct evaluation is presented in [26], [27], [28], [29], [30].

6 Passing from an Isolated Defect to Consecutive Defects of a Track

The first term in the bracket of Eqn (5.9) is depicted on the vertical axis [y] while on the horizontal axis [x] the percentages of the wavelength μ·λ are shown. We observe that z(x) has its maximum value for $T_1/T_n=0{,}666667=2/3$, equal to 1,465:

$$z(t)=\left[\frac{m_{NSM}}{(m_{NSM}+m_{TRACK})}\right]\cdot\alpha\cdot 1{,}465 \qquad (6.1)$$

for $x=0.91\lambda$. The relation T_1/T_n represents the cases for short and long wavelength of the defects. For $T_1/T_n=2$-$2{,}5$ the wavelength is long and for T_1/T_n << the wavelength is short ([7], p.49). The second derivative of z(x) from Eqn (5.7), that is the vertical acceleration that gives the dynamic overloading due to the defect, is calculated, see the following **Eqn:**

$$z''(t)=-\frac{\alpha}{2}\cdot\frac{m_{NSM}}{(m_{NSM}+m_{TRACK})}\cdot\frac{1}{1-\left(\frac{\omega_n}{\omega_1}\right)^2}\cdot\left[\underbrace{\omega_1^2\cdot\cos(\omega_1 t)}_{steady-state}-\underbrace{\omega_n^2\cdot\cos(\omega_n t)}_{transient-part}\right]$$

(6.2a)

$$z'(t)=\frac{\alpha}{2}\cdot\frac{m_{NSM}}{(m_{NSM}+m_{TRACK})}\cdot\frac{1}{1-\left(\frac{\omega_n}{\omega_1}\right)^2}\cdot\left[\underbrace{-\omega_1\cdot\sin(\omega_1 t)}_{steady-state}+\underbrace{\omega_n\cdot\sin(\omega_n t)}_{transient-part}\right]$$

(6.2b)

for discrete values of $n=\omega_n/\omega_1$ ($=T_1/T_n$) and μ a percentage of the wavelength λ, and $T_n=0{,}0307$ sec as calculated above. The additional subsidence of the deflection z at the beginning of the defect is negative in the first part of the defect. Following the wheel's motion, z turns to positive sign and reaches its maximum and possibly afterwards z becomes again negative. After the passage of the wheel over the defect, one oscillation occurs which approaches to the natural cyclic frequency ω_n (this oscillation is damped due to non-existence of a new defect since we considered one isolated defect) in reality, even if in the present analysis the damping was omitted for

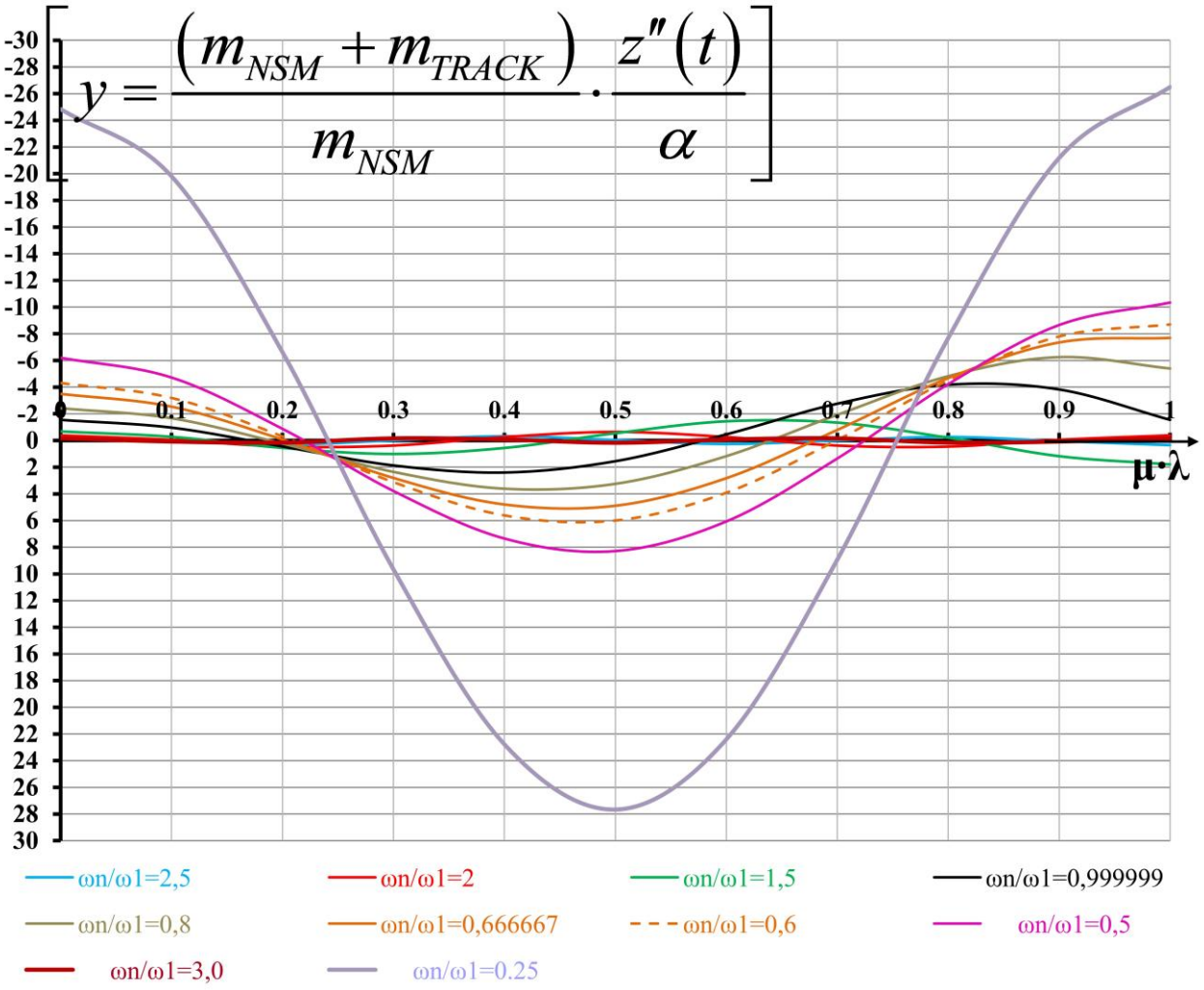

Figure 7. Depicting Eqn (7.1a) on a graph (in a scale). For the vertical acceleration [z″] due to a defect of short or long wavelength: in the Horizontal Axis [x] the percentage of the wavelength λ of the defect is depicted. In the Vertical Axis [y] the first term of Eqn (7.1a), in the brackets, is depicted.

simplicity. The values of the calculations of both Fig.6 and Fig.7 are presented in Annex 2.

7 Parametric Analysis of Short and Long Wavelength Defects

If, now, we consider a long wavelength defect with a wavelength that produces a forced oscillation with:

$\frac{T_1}{T_n} = \frac{\omega_n}{\omega_1} = 2,5$, we calculate (in Fig. 8 is 0,19, for x=0,41·λ): $z_{\max} = \left| \frac{m_{NSM} \cdot \alpha \cdot 0,19}{(m_{NSM} + m_{TRACK})} \right| = 0,133 \cdot \alpha$

with the values calculated above: T_n = 0,026 sec, T_1 = 0,065 sec, the wavelength λ equals:

$$\lambda = V \cdot T_1 = 2,5 \cdot V \cdot T_n = 0,065 \cdot 57,69 = 3,75m$$

This value represents a defect of adequately long wavelength. The static deflection due to a wheel load of 11,25 t or 112,5 kN is equal to:

$$\left| \frac{(m_{NSM} + m_{TRACK})}{m_{NSM}} \cdot \frac{z''(t)}{\alpha} \right| =$$

$$-\frac{1}{2} \cdot \frac{\omega_1^2}{1 - \left(\frac{\omega_n}{\omega_1}\right)^2} \cdot \left| \underbrace{\cos\left(\frac{2\pi V}{\lambda} \cdot \frac{\mu \cdot \lambda}{V}\right)}_{steady-state} - \underbrace{\frac{\omega_n^2}{\omega_1^2} \cdot \cos\left(n \cdot \frac{2\pi V}{\lambda} \frac{\mu \cdot \lambda}{V}\right)}_{transient-part} \right| =$$

$$= \frac{112.500N}{2\sqrt{2}} \cdot 1,524228617 \cdot 10^{-5} \frac{mm}{N} = 0,606mm \textbf{(7.1a)}$$

Consequently, for α=1 mm, that is for every mm of vertical defect, the dynamic increment of the static deflection is equal to (0,133/0,606)=21,9% of the static deflection (for every mm of the depth of the defect).

If we examine the second derivative (vertical acceleration) as a percentage of g, the acceleration of gravity, then [from Eqn (6.2a-b)]:

$$z_{static} = \frac{Q_{wheel}}{2\sqrt{2}} \cdot \sqrt[4]{\frac{\ell^3}{EJ\rho_{total}^3}} =$$

$$= \frac{112.500N}{2\sqrt{2}} \cdot \sqrt[4]{\frac{600^3 mm^3}{210.000\frac{N}{mm^2} \cdot 3{,}06 \cdot 10^7 mm^4 \cdot 85.396^3 \frac{N^3}{mm^3}}} =$$

$$= -\left(\frac{2\pi}{n \cdot T_n}\right)^2 \cdot \frac{1}{g} \cdot \left| \frac{1}{2 \cdot \left[1-(n)^2\right]} \cdot \left| \underbrace{\cos(2\pi\mu)}_{steady-state} - \underbrace{(n)^2 \cdot \cos(2n\pi\mu)}_{transient-part} \right| \right| \quad [\%g]$$

(**7.1b**)

Equation (7.1a) is plotted in Fig. 7.

The first term in the bracket of Eqn (7.1a) is depicted on the vertical axis [y] while on the horizontal axis [x] the percentages of the wavelength $\mu \cdot \lambda$ are shown. For the case calculated above in Fig. 6, at the point x=0,41·λ the term in bracket has a value of -0,332:

$$\left| \frac{(m_{NSM} + m_{TRACK})}{m_{NSM}} \cdot \frac{1}{g} \cdot \frac{z''(t)}{\alpha} \right| = -0.332041 \Rightarrow$$

$$z''(t) = -0.332041 \cdot \frac{1{,}0}{1{,}0 + 0{,}426} \cdot g \cdot \alpha = 0{,}233 \cdot g \cdot \alpha$$

Eqn (5.3) (its second part corresponds to the static action of the wheel load) has as particular solution:

$$z = \frac{m_{NSM} \cdot g}{h_{TRACK}}$$

Abandoning the second part leads to the classic solution where z is the supplementary subsidence owed to the dynamic increase of the Load. The dynamic increase of the Load is equal to:

$$Q_{dynamic} = h_{TRACK} \cdot z + m_{TRACK} \cdot z'' =$$

$$= 85.396 \cdot 0{,}133 - 426kg \cdot 0{,}233 \cdot 9{,}81 \frac{m}{\sec^2} =$$

$$= 1{,}04t \qquad (7.2)$$

where, from the analysis above: h_{TRACK} = 8539,6 t/m = 85.396 N/mm, m_{TRACK} = 0,426 t = 426 kg. Consequently, for arc height (i.e. sagitta) α=1 mm of a defect of wavelength λ, that is for every mm of vertical defect, the dynamic increase of the load is equal to (1,04/ 11,25)=9,24% of the static load of the wheel (for every mm of the depth of the defect). Apparently the increase of the static stiffness coefficient and of the inferred dynamic stiffness coefficient of track leads to lower values of $Q_{dynamic}$ since the h_{TRACK} is in the denominator in the equation for calculation of *z*, consequently the first term of the Eqn (23) for the $Q_{dynamic}$ will be reduced. The same happens for the track mass participating in the motion of the Non-Suspended Masses of the wheel. Thus finally the $Q_{dynamic}$ will be reduced when the ρ_{total} and the h_{TRACK} are increased.

In the case of a defect of long wavelength, when the speed V increases, then T_1 decreases and the supplementary subsidence, owed to the dynamic increase of the load, increases; consequently the dynamic component of the load due to the Non-Suspended Masses increase more rapidly since it depends on ω_1^2 , that is on the square of the speed V. When the dynamic rigidity $h_{TRACK}=\rho_{dynamic}$ increases, then the eigenperiod T_n decreases and T_1/T_n increases and the supplementary subsidence, owed to the dynamic increase of the load, decreases for the same speed V; one higher rigidity (stiffness coefficient) is still advantageous. For defects of longer wavelength, the oscillations of the Suspended Masses become predominant since the oscillations of the Non-Suspended Masses decrease.

The results presented so far and the arithmetic comparisons give an idea and enlighten the influence of some kinds of track defects as well as of several parameters, but the calculations do not take into account the amortization of the oscillations due to the damping of the track and mainly of the ballast, consequently the derived arithmetic values are larger than the real values. For example in the case of the theoretical calculation of the track mass which participates in the motion of the Non-Suspended Masses of the railway vehicles without damping give results 33% larger than the real ones since if we take into account the damping coefficient of the track the variation between the results of the theoretical calculations and the real values measured on track fluctuates between 0,5 and 4% ([14]; compared to [13]), fact depicting the accuracy of the theoretical calculations, if the totality of the parameters is taken into account.

8 Summary - Conclusions

The basic concept for this article resulted during the theoretical and experimental investigation which took place under the cooperation among experts of OSE[1] and SNCF[2] (1988-1989) [[32], [33], [21]] and personal research of the author either in the Hellenic Railways Organization (OSE) or at the University of Thessaly, Civil Engineering Department (2007-2014) but also later until now (2025).

We should underline that *the present article investigates with accurate mathematical calculations -in more depth and in more details-,* the values of both z and z″ of the Eqns (5.9) and (7.1a), than the

[1] Initials of the Hellenic Railways Organization in Greek.

[2] Initials of the French State Railways in French.

[31] and [30] did. The graphs of Figs 6, 7 are in a scale that permits easy interpolation to find the values of the parameters. We remark now in the present article that as the ω_n/ω_1 decreases, then *-in absolute values-* the values of the y-axis increase in Fig.6, but up to an upper limit (see Annex 2), since in Fig.7 they increase significantly; that's why we did not proceed the calculations to values <0.05 in Annex 2, but till 0.25 in Fig.7. After detailed calculations, we also remark that, as the relation ω_n/ω_1 increases, the values of y-axis in both Figs 6, 7 tend to fluctuate around zero, that's why we restricted the calculations for ω_n/ω_1 up to 2.5 in Fig.6 and 3 in Fig.7.

General Ascertainments resulting from the present article but also from [31] and [30]:

For a defect of long wavelength λ and sagitta of 1 mm (depth of the defect), the dynamic increase of the acting load –compared to the static wheel load– is equal to 9,24%. Furthermore, from Fig. 6 and Fig. 7, it is verified that when the speed increases, the period T_1 decreases and the supplementary sagitta (depth of the defect) increases. Supplementary, since it is added to the static deflection and it is owed to the dynamic component of the load. The increase of the dynamic component of the load increases faster since it is dependent on the square of the speed $(\omega_1)^2$. When the dynamic stiffness coefficient h_{TRACK} increases, T_n decreases, T_1/T_n increases, the supplementary sagitta decreases (for the same V), and the dynamic component of the action decreases also. Furthermore, in the case of longer wavelengths the oscillations of the Suspended Masses become predominant since the oscillations of the Non-Suspended Masses decrease.

Consequently, the softer the pad and/or the subgrade (subgrade and prepared subgrade) then the higher percentage of the load is transmitted through the sleeper to the substructure of the railway track under the running load/axle. Finally in total, the reaction per support point of the rail/sleeper, in the case of softer pads and more resilient fastenings, is smaller due to a distribution of the load along the track in more support points of the rail/sleepers, as it can be derived from literature ([1]; [6]; [2]). In the case of the short wavelength defects this is more clearly verified.

For defects of very long wavelength, the oscillations of the Suspended Masses become predominant since the oscillations of the Non-Suspended Masses decrease.

References

[1]. Giannakos, K., and, A. Loizos. 2010. Evaluation of actions on concrete sleepers as design loads – Influence of fastenings, International Journal of Pavement Engineering (IJPE), Vol. 11, Issue 3, June, 197 – 213.

[2]. Giannakos, K. 2010a. Loads on track, Ballast Fouling and Life-cycle under Dynamic Loading in Railways, International Journal of Transportation Engineering – ASCE, Vol. 136, Issue 12, 1075-1084.

[3]. Giannakos, K. 2015. Modeling the Influence of Short Wavelength Defects in a Railway Track on the Dynamic Behavior of the Non-Suspended Masses, Journal Mechanical Systems and Signal Processes (jmssp), Elsevier, 68-69, (2016), 68-83, http://dx.doi.org/10.1016/j.ymssp.2015.07.020.

[4]. Winkler, E. 1867. Die Lehre von der Elastizität und Festigkeit (The Theory of Elasticity and Stiffness), H. Dominicus, Prague.

[5]. Zimmermann, H. 1941. Die Berechnung des Eisenbahnoberbaues, Verlag von Wilhelm Ernst & Sohn, Berlin.

[6]. Giannakos, K.2004. Actions on the Railway Track, Papazissis publications, Athens, Greece, http://www. papazisi.gr.

[7]. Alias, J. 1984. La Voie Ferree, IIeme edition, Eyrolles, Paris.

[8]. Eisenmann, J. 1988. Schotteroberbau – Moglichkeiten und Perspektiven fur die Moderne Bahn, Die Naturstein-Industrie, Heft 3, (Isernhagen, Germany), 6-11 (1988).

[9]. Giannakos, K. 2013a. Ties' Design in High -Speed and Heavy Haul Railroads: Ultimum Strength vs Actions on Track, presented in the workshop for sleepers and fastenings of TRB, 92nd Annual Meeting, proceedings.

[10]. Giannakos, K. 2013b. Selected Topics in Railway Engineering, University of Thessaly, Dpt. Civil Engineering, Greece, www.uth.gr.

[11]. Jenkins, H., J., Stephenson, G., Clayton, G., Morland, and, D., Lyon. 1974. Incidences des parametres carac-teristigues de la voie et des vehicules sur les efforts dynamigues verticaux gui se developpent entre rail et roue, *Rail International 10/(1974)*, 682-702.

[12]. SNCF. 1981. Mecanique de la voie.

[13]. Giannakos, K.2010b. Theoretical calculation of the track-mass in the motion

of unsprung masses in relation to track dynamic stiffness and damping, International Journal of Pavement Engineering (IJPE) - Special Rail Issue: "High-Speed Railway Infrastructure: Recent Developments and Performance", Vol. 11, number 4, p. 319-330, August.

[14]. Giannakos, K. 2012. Influence of the Track's Damping on the Track Mass Participating in the Motion of the Non Suspended Masses of Railway Vehicles-Theoretical Calculation and Comparison to Measurements, volume published in honor of professor G. Giannopoulos, Aristotle University of Thessaloniki.

[15]. Fortin, J. 1982. La Deformee Dynamique de la Voie Ferree, RGCF, 02/1982.

[16]. Thompson, D. 2009. Railway Noise and Vibration, Elsevier.

[17]. SNCF/Direction de l' Equipement. 1981. Mecanique de la Voie, Paris.

[18]. Prud'homme, A. 1969/1966. Sollicitations Statiques et Dynamiques de la Voie, SNCF/ Direction des Installations Fixes, Paris.

[19]. Chopra, A. 2001. Dynamics of Structures – Theory and Applications to Earthquake Engineering, Prentice Hall, second edition, USA.

[20]. Argyris, J., and, H.-P., Mlejnek. 1991. Texts on Computational Mechanics, Volume V Dynamics of Structures, North-Holland, Elsevier, New York, USA.

[21]. OSE/SNCF, Cooperation. 1988. Comportment des traverses en relation avec les charges dynamiques, June.

[22]. Max, J. 1985. Methodes et Techniques de Traitement du Signal et Applications aux Measures Physiques, Masson, Paris.

[23]. Young, H.J. 1992. Physics, greek edition, vols I, II, Papazisis publications, Athens, 1994; Addison-Wesley.

[24]. Giannakos, K., S., Tsoukantas, A., Sakareli, and, C., Zois.2011. Schwankung des Steifigkeit zwischen Fester Fahrbahn und Schottergleis - Beschrieben wird die parametrische Analyse der Schwankung des Steifigkeitsfaktors im Übergangsbereich zwischen Fester Fahrbahn und Schottergleis, EI - Eisenbahningenieur, Germany, February 2011, 12-19.

[25]. Giannakos, K., and, S., Tsoukantas. 2010. Requirements for Stiffness Variation between Slab and Ballasted Railway Track and Resulting Design Loads, ICASTOR (Indian Centre For Advanced Scientific and Technological Research) Journal for Engineering, January 2010, Vol.3, No 1 (2010), 21 - 35.

[26]. Giannakos, K. 2023. Influence of Track Defects on the Track-Loads and Confidence Interval of a Track Recording Car, WSEAS Transactions on Applied and Theoretical Mechanics, Vol. 18, 2023, 16-31, https://wseas.com/journals/mechanics/2023-a065111-001(2023).pdf.

[27]. Giannakos, K. 2024. Railway System 'Vehicle-Track': Relation Between the Spectral Density of Excitation vs of Response, International Journal of Mechanical Engineering, Vol.9, 1-14. https://www.iaras.org/home/caijme/railway-system-vehicle-track-relation-between-the-spectral-density-of-excitation-vs-of-response.

[28]. Giannakos, K. 2025a. Railway System 'Vehicle-Track': Simulation, Mathematical Modelling and Spectral Densities of Excitation and Response (Part II), International Journal of Mechanical Engineering, Vol. 10, 56-74. https://www.iaras.org/home/caijme/railway-system-vehicle-track-simulation-mathematical-modelling-and-spectral-densities-of-excitation-and-response-part-ii.

[29]. Giannakos, K. 2025b. Utilization of the Spectral Density -derived From the Recordings of the Random Defects on a Railway Track- in the Maintenance Works, International Journal of Mechanical Engineering, Vol. 10, 83-102, International Journal of Mechanical Engineering http://www.iaras.org/iaras/journals/ijme.

[30]. Giannakos, K. 2022. Control of the Geometry of a Railway Track: Measurements of Defects and Theoretical Simulation, *International Journal on Applied Physics and Engineering*, Vol.1, 102-115.

[31]. Giannakos, K. 2014. Actions on a Railway Track, due to an Isolated Defect, International Journal of Control and Automation, Vol.7, No.3, 195-212.

[32]. Giannakos, K., Domsa-Vlassopoulou, I., and, P., Iordanidis. 1988. Έκθεση Επιτροπής Εμπειρογνωμόνων του ΟΣΕ για την Επίσκεψη στους SNCF ap;ο 15/5/1988-11/6/1988, Αθήνα.
[33]. Giannakos, K., Domsa-Vlassopoulou, I., and, P., Iordanidis. 1989. Πρακτικά Συναντήσεων κατά τη Συνεργασία με τους SNCF στο Παρίσι-St Ouen, Παρίσι/Αθήνα.

ANNEX 1

In the case of a free oscillation (without external force) the equation is:

$$m\cdot\ddot{z}+k\cdot z=0\Rightarrow\ddot{z}+\frac{k}{m}\cdot z=0\Rightarrow\ddot{z}+\omega_n^2\cdot z=0 \quad (1.1)$$

The general solution is [4]:

$$z(t)=A\cdot\cos(\omega_n t)+B\cdot\sin(\omega_n t)\Rightarrow$$

$$z(t)=z(0)\cdot\cos(\omega_n t)+\frac{\dot{z}(0)}{\omega_n}\cdot\sin(\omega_n t) \quad (1.2)$$

Where:

$$A=z(0),\quad B=\frac{\dot{z}(0)}{\omega_n} \quad (1.3.)$$

If we pass to the undamped harmonic oscillation of the form:

$$m\cdot\ddot{z}+k\cdot z=p_0\cdot\cos(\omega t)\Rightarrow$$

$$\ddot{z}+\omega_n^2\cdot z=\frac{p_0}{m}\cdot\cos(\omega t)\Rightarrow \quad (1.4)$$

$$\ddot{z}+\omega_n^2\cdot z=\omega_n^2\cdot\frac{p_0}{k}\cdot\cos(\omega t)$$

where:

$$\omega_n^2=\frac{k}{m}\Rightarrow m=\frac{k}{\omega_n^2} \quad (1.5)$$

The particular solution of the linear second order differential equation (1.4) is of the form:

$$z_p(t)=C\cdot\cos(\omega t)\Rightarrow$$
$$\dot{z}_p(t)=-\omega\cdot C\cdot\sin(\omega t)\Rightarrow \quad (1.6)$$
$$\ddot{z}_p(t)=-\omega^2\cdot C\cdot\cos(\omega t)$$

Substituting equation (1.6) to equation (1.4) we derive:

$$-\omega^2\cdot C\cdot\cos(\omega t)+\omega_n^2\cdot C\cdot\cos(\omega t)=\frac{p_0}{m}\cdot\cos(\omega t)\Rightarrow$$

$$-\omega^2\cdot C+\omega_n^2\cdot C=\omega_n^2\cdot\frac{p_0}{k}\Rightarrow$$

$$\dot{z}(0)=-\omega_n\cdot A\cdot\sin(0)+\omega_n\cdot B\cdot\cos(0)-\frac{p_0}{k}\cdot\frac{\omega}{1-\left(\frac{\omega}{\omega_n}\right)^2}\cdot\sin(0)\Rightarrow \quad (1.7)$$

$$B=\frac{\dot{z}(0)}{\omega_n}$$

The general solution for the equation (1.4) is the addition of the solution (1.2) and of the solution of the equation (1.6) combined with equation (1.7):

$$z(t)=A\cdot\cos(\omega_n t)+B\cdot\sin(\omega_n t)+\frac{p_0}{k}\cdot\frac{1}{1-\left(\frac{\omega}{\omega_n}\right)^2}\cdot\cos(\omega t) \quad (1.8)$$

$$\dot{z}(t)=-\omega_n\cdot A\cdot\sin(\omega_n t)+\omega_n\cdot B\cdot\cos(\omega_n t)-$$
$$-\frac{p_0}{k}\cdot\frac{\omega}{1-\left(\frac{\omega}{\omega_n}\right)^2}\cdot\sin(\omega t) \quad (1.9)$$

Calculating the values of equation (1.8) and (1.9) at t=0:

$$z(0)=A\cdot\cos(0)+B\cdot\sin(0)+\frac{p_0}{k}\cdot\frac{1}{1-\left(\frac{\omega}{\omega_n}\right)^2}\cdot\cos(0)\Rightarrow \quad (1.10)$$

$$A=z(0)-\frac{p_0}{k}\cdot\frac{1}{1-\left(\frac{\omega}{\omega_n}\right)^2}$$

$$z(t)=\underbrace{\left[z(0)-\frac{p_0}{k}\cdot\frac{1}{1-\left(\frac{\omega}{\omega_n}\right)^2}\right]}_{transient-part}\cdot\cos(\omega_n t)+\frac{\dot{z}(0)}{\omega_n}\cdot\sin(\omega_n t)+ \quad (1.11)$$
$$+\frac{p_0}{k}\cdot\frac{1}{1-\left(\frac{\omega}{\omega_n}\right)^2}\cdot\cos(\omega t)$$

$$C\left(\omega_n^2-\omega^2\right)=\omega_n^2\cdot\frac{p_0}{k}\Rightarrow$$

$$C=\frac{\omega_n^2}{\left(\omega_n^2-\omega^2\right)}\cdot\frac{p_0}{k}\Rightarrow C=\frac{p_0}{k}\cdot\frac{1}{1-\left(\frac{\omega}{\omega_n}\right)^2} \quad (1.12)$$

and for initial conditions z(0)=ż(0)=0:

$$z(t)=\frac{p_0}{k}\cdot\frac{1}{1-\left(\frac{\omega}{\omega_n}\right)^2}\cdot\left[\underbrace{\cos(\omega t)}_{steady-state}-\underbrace{\cos(\omega_n t)}_{transient-part}\right] \quad (1.13)$$

ANNEX 2 – Calculations of Figs 6, 7

Calculations of Figure 6

	ω_n/ω_1=2		ω_n/ω_1=2,5		ω_n/ω_1=1,5		ω_n/ω_1=0,999999		ω_n/ω_1=3	
	x	y	x	y	x	y	x	y	x	y
0	0	0	0	0	0	0	0	0	0	0
0,1λ	0.1	-0.08333	0.1	-0.07705	0.1	-0.08849	0.1	-0.09233	0.1	-0.069877
0,2λ	0.2	-0.18634	0.2	-0.12467	0.2	-0.24721	0.2	-0.29878	0.2	-0.069877
0,3λ	0.3	-0.08333	0.3	0.02943	0.3	-0.25682	0.3	-0.44818	0.3	0.069877
0,4λ	0.4	0.186339	0.4	0.172287	0.4	0	0.4	-0.36932	0.4	0.069877
0,5λ	0.5	0.333333	0.5	0.095238	0.5	0.4	0.5	-1E-06	0.5	0
0,6λ	0.6	0.186339	0.6	-0.01819	0.6	0.647214	0.6	0.553973	0.6	0.069877
0,7λ	0.7	-0.08333	0.7	0.02943	0.7	0.504029	0.7	1.045741	0.7	0.069877
0,8λ	0.8	-0.18634	0.8	0.065808	0.8	0	0.8	1.195134	0.8	-0.069877
0,9λ	0.9	-0.08333	0.9	-0.07705	0.9	-0.55872	0.9	0.830965	0.9	-0.069877
1,0λ	1	0	1	-0.19048	1	-0.8	1	0.000005	1	0

Calculations of Figure 6

	ω_n/ω_1=0,8		ω_n/ω_1=0,666667		ω_n/ω_1=0,6		ω_n/ω_1=0,5		ω_n/ω_1=0,25		ω_n/ω_1=0,10		ω_n/ω_1=0,05	
	x	y	x	y	x	y	x	y	x	y	x	y	x	y
0	0	0	0	0	0	0	0	0	0	0	0	0	0	0
0,1λ	0.1	-0.09346	0.1	-0.09408	0.1	-0.09434	0.1	-0.09469	0.1	-0.095291	0.1	-0.095459	0.1	-0.095483
0,2λ	0.2	-0.31501	0.2	-0.3241	0.2	-0.32809	0.2	-0.33333	0.2	-0.342421	0.2	-0.344999	0.2	-0.345368
0,3λ	0.3	-0.5164	0.3	-0.55623	0.3	-0.57406	0.3	-0.59787	0.3	-0.640013	0.3	-0.652174	0.3	-0.653924
0,4λ	0.4	-0.53228	0.4	-0.63404	0.4	-0.6811	0.4	-0.74536	0.4	-0.862951	0.4	-0.897778	0.4	-0.902823
0,5λ	0.5	-0.26525	0.5	-0.45	0.5	-0.53983	0.5	-0.66667	0.5	-0.910457	0.5	-0.985382	0.5	-0.9996335
0,6λ	0.6	0.254302	0.6	0	0.6	-0.13406	0.6	-0.33333	0.6	-0.744961	0.6	-0.878179	0.6	-0.897897
0,7λ	0.7	0.862166	0.7	0.602218	0.7	0.443195	0.7	0.185846	0.7	-0.406947	0.7	-0.613053	0.7	-0.644077
0,8λ	0.8	1.314501	0.8	1.158448	0.8	1.016509	0.8	0.745356	0.8	0	0.8	-0.28651	0.8	-0.33061
0,9λ	0.9	1.383887	0.9	1.456231	0.9	1.38875	0.9	1.173382	0.9	0.348044	0.9	-0.017834	0.9	-0.075828
1,0λ	1	0.959699	1	1.35	1	1.413295	1	1.333333	1	0.533333	1	0.096456	1	0.024533

Calculations of Figure 7

z''	ω_n/ω_1=2		ω_n/ω_1=2,5		ω_n/ω_1=1,5		ω_n/ω_1=0,999999	
	x	y	x	y	x	y	x	y
0	0	-0.38815	0	-0.24841	0	-0.69004	0	-1.55259
0,1λ	0.1	-0.05525	0.1	0.03828	0.1	-0.28347	0.1	-0.96937
0,2λ	0.2	0.458671	0.2	0.310352	0.2	0.554407	0.2	0.447997
0,3λ	0.3	0.378708	0.3	-0.01462	0.3	1.010691	0.3	1.871438
0,4λ	0.4	-0.2646	0.4	-0.33401	0.4	0.558253	0.4	2.402865
0,5λ	0.5	-0.64691	0.5	-0.04732	0.5	-0.55203	0.5	1.552593
0,6λ	0.6	-0.2646	0.6	0.257451	0.6	-1.45146	0.6	-0.46411
0,7λ	0.7	0.378708	0.7	-0.01462	0.7	-1.35187	0.7	-2.76743
0,8λ	0.8	0.458671	0.8	-0.28111	0.8	-0.21323	0.8	-4.19088
0,9λ	0.9	-0.05525	0.9	0.03828	0.9	1.176672	0.9	-3.83636
1,0λ	1	-0.38815	1	0.343048	1	1.7941	1	-1.55261

Calculations of Figure 7

z''	ω_n/ω_1=0,8		ω_n/ω_1=0,666667		ω_n/ω_1=0,6		ω_n/ω_1=0,5		ω_n/ω_1=3,0		ω_n/ω_1=3.5		ωn/ω1=0.25		ωn/ω1=0.05	
	x	y	x	y	x	y	x	y	x	y	x	y	x	y	x	y
0	0	-2.42592	0	-3.49332	0	-4.31274	0	-6.21035	0	-0.17250958	0	-0.126741734	0	24.8414	0	-0.12674173
0,1λ	0.1	-1.6724	0.1	-2.53403	0.1	-3.19613	0.1	-4.73024	0.1	0.07741734	0.1	0.090233201	0.1	19.8012	0.1	0.090233201
0,2λ	0.2	0.228522	0.2	-0.0731	0.2	-0.31394	0.2	-0.88405	0.2	0.16367213	0.2	0.046128078	0.2	6.61313	0.2	0.046128078
0,3λ	0.3	2.353158	0.3	2.806685	0.3	3.115264	0.3	3.775586	0.3	-0.16367213	0.3	-0.134734454	0.3	9.663758	0.3	-0.13473445
0,4λ	0.4	3.615412	0.4	4.794953	0.4	5.604011	0.4	7.338734	0.4	-0.07741734	0.4	0.102536216	0.4	22.77671	0.4	0.102536216
0,5λ	0.5	3.249576	0.5	4.890642	0.5	5.989006	0.5	8.28046	0.5	0.172509582	0.5	-0.011265932	0.5	27.66851	0.5	-0.01126593
0,6λ	0.6	1.172955	0.6	2.82615	0.6	3.90535	0.6	6.059332	0.6	-0.07741734	0.6	-0.120764877	0.6	22.41033	0.6	-0.12076488
0,7λ	0.7	-1.92753	0.7	-0.7905	0.7	-0.04349	0.7	1.34202	0.7	-0.16367213	0.7	0.127771725	0.7	8.940018	0.7	0.127771725
0,8λ	0.8	-4.8314	0.8	-4.67668	0.8	-4.48915	0.8	-4.23356	0.8	0.16367213	0.8	-0.03916535	0.8	-7.67641	0.8	-0.03916535
0,9λ	0.9	-6.25981	0.9	-7.348	0.9	-7.80139	0.9	-8.66783	0.9	0.07741734	0.9	-0.07200454	0.9	-21.1778	0.9	-0.07200454
1,0λ	1	-5.40595	1	-7.6853	1	-8.70126	1	-10.3506	1	-0.17250958	1	0.149273597	1	-26.4975	1	0.149273597